Available online at www.sciencedirect.com
SCIENCE DIRECT®
Chemical Physics Letters 392 (2004) 314–318
CHEMICAL PHYSICS LETTERS
www.elsevier.com/locate/cplett

Electric and magnetic-field tuning of tubular image states above suspended nanowires

Dvira Segal *, Petr Král, Moshe Shapiro

Department of Chemical Physics, Weizmann Institute of Science, 76100 Rehovot, Israel
Departments of Chemistry and Physics, The University of British Columbia, Vancouver, BC, Canada V6T1Z1

Received 9 April 2004; in final form 20 May 2004

Abstract

Recently, we have shown that suspended metallic nanowires support Rydberg-like electron image states. Here, we investigate the possibility of tuning such 'tubular image states', formed around *pairs* of parallel nanowires, by electric and magnetic fields. In the presence of a magnetic field, directed along the nanowires, we observe the formation of 'Landau-like' image states, with simple elliptic-like orbits, that are highly detached from the surfaces of *both* nanowires. An additional electric field, induced by opposite charging of the two nanowires, spatially shifts these 'molecular' states to one of the wires, while strongly chaotic nodal patterns emerge.

1. Introduction

Rydberg states in atomic [1] and molecular systems [2] are largely tunable by electric and magnetic fields. The field-induced symmetry breaking of the electron confining potentials leads to a number of interesting phenomena [3], that range from a simple levels repulsion to intriguing transitions from regular to irregular energy spectra and chaotic dynamics [4–6]. From the point of possible applications, it would be also interesting to prepare such extended states with prolongated lifetimes above solid-state nanosystems.

Recently, we have shown that suspended nanowires, such as a metallic carbon nanotubes, support Rydberg-like electron image states, that can be largely detached from the material surfaces, due to the existence of angular momentum barriers [7]. We have described transversal and longitudinal shaping of these 'tubular image states' (TIS) above inhomogeneous nanowires [8] and demonstrated the formation of image-state bands above periodical arrays of nanowires [9].

In this work, we examine the possibility of manipulating image states, formed in the vicinity of two (or more) parallel nanowires, by external electric and magnetic fields. We focus our study on the facile field-induced tunability of these states, and in particular, their collapse or detachment from the tubes, and related emergence of chaos in the system.

In Fig. 1, we show the scheme of our system, comprised of two parallel metallic nanotubes. Their long axis is aligned along the z-direction and their centers are placed at the $x = \pm d/2$, $y = 0$ positions. We can positively charge one nanotube and negatively charge the other, while keeping the overall pair charge neutral, thus creating an electric field directed in the x–y plane (i.e., the two tubes have the added potentials $\pm V_a$). In addition, we apply an external magnetic field aligned along the z-direction. The external fields can be applied analogously in arrays of nanotubes [9].

2. The model system

The correlated electron gas in metallic carbon nanotubes has a screening length of the order of the nanotube's radius [10]. Since the image states are sepa-

* Corresponding author. Fax: +972-8-9344123.
E-mail address: dvira.segal@weizmann.ac.il (D. Segal).

0009-2614/$ - see front matter © 2004 Elsevier B.V. All rights reserved.
doi:10.1016/j.cplett.2004.05.075

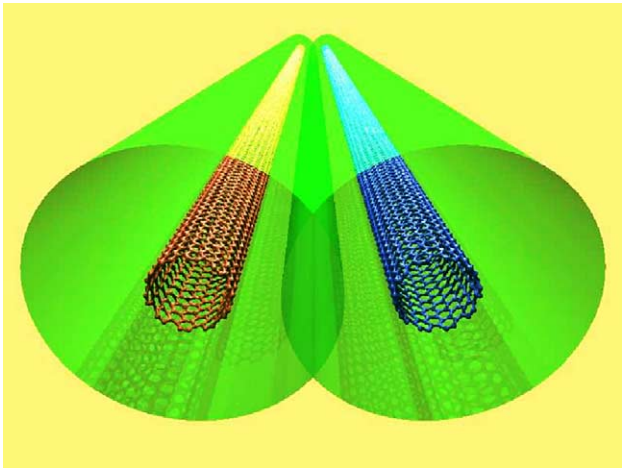

Fig. 1. Control of tubular image states in the vicinity of two parallel nanotubes. The states are tunned by opposite charging of the tubes and by application of a magnetic field, aligned along their long axis.

rated to large distances from the tube's center, we can model the tube (nanowire) by an ideally conducting cylinder of radius a [7,11]. An external electron placed at a distance r from the cylinder's center is electrostatically attracted to the image charge induced in its surface. For an infinitely long wire, the screening potential can be calculated analytically and expressed in terms of regular and irregular Bessel functions [7]. From the exact solution, we can find an approximate expression

$$V_{\mathrm{s}}(r) \approx \frac{2e^2}{\pi a} \sum_{n=1,3,5,\ldots} \mathrm{li}[(a/r)^n], \quad \mathrm{li}(x) \equiv \int_0^x \frac{\mathrm{d}t}{\ln(t)}, \tag{1}$$

interpolating well the long-range $-e^2/(r\ln(r/a))$ and the near-surface $1/(|r-a|)$ behavior.

The electron also interacts with homogeneously spread charges, due to the $\pm V_{\mathrm{a}}$ potential applied on each of the tubes. Since the tubes are relatively far apart from each other, i.e., $d \gg a$, we can assume that they do not polarize each other. In this case the additional potential energy of an electron placed at r_1 and r_2 away from the centers of the two tubes, due to the charging of the tubes, is given by [11]

$$V_{\mathrm{C}}(r_1, r_2) \approx eV_{\mathrm{a}} \frac{\ln(r_1/r_2)}{\ln(2a/d)}. \tag{2}$$

This formula goes over to the correct limit of $\pm eV_{\mathrm{a}}$ when the electron is placed on the surface of one of the tubes, i.e., when $r_1 = a$ and $r_2 = d/2$ and vice versa. Neglecting the short-range terms arising from multiple reflections of image charges belonging to different nanotubes, the total potential energy of the external electron is given as $V_{\mathrm{T}}(r_1, r_2) = V_{\mathrm{s}}(r_1) + V_{\mathrm{s}}(r_2) + V_{\mathrm{C}}(r_1, r_2)$.

We also apply a uniform magnetic field $\mathbf{B}$ to the system, that is oriented along the z-axis of the tubes. Thus, the total Hamiltonian is given as,

$$H = \frac{1}{2m_{\mathrm{e}}}(\mathbf{p} - e\mathbf{A})^2 + V_{\mathrm{T}}(x, y), \tag{3}$$

where $\mathbf{A} = (B/2)(-y, x, 0)$ is the vector potential of the field in the Landau gauge, and $\mathbf{p}$ is the generalized momentum of the electron. It gives rise to two additional terms in the Hamiltonian (3)

$$H_1 = -\frac{eB}{2m_{\mathrm{e}}} L_z, \quad H_2 = \frac{e^2B^2}{8m_{\mathrm{e}}}(x^2 + y^2), \tag{4}$$

$$\text{where} \quad L_z = -\mathrm{i}\hbar\left(x\frac{\partial}{\partial y} - y\frac{\partial}{\partial x}\right)$$

is the angular momentum operator, and m_{e} is the electron mass. In what follows we ignore the electron spin.

The image-state wavefunctions are separable in the z coordinate, $\Psi(x, y, z) = \psi_v(x, y)\,\phi_{k_z}(z)$, and their energies are given as, $E_v + \epsilon_{k_z}$. The $\psi_v(x, y)$ components fulfill the Schrödinger equation

$$\left\{\frac{-\hbar^2}{2m_{\mathrm{e}}}\left(\frac{\partial^2}{\partial x^2} + \frac{\partial^2}{\partial y^2}\right) + V_{\mathrm{T}}(x, y) + H_1(x, y) + H_2(x, y) - E_v\right\}\psi_v(x, y) = 0. \tag{5}$$

We solve Eq. (5) numerically, using a multidimensional discrete variable representation (DVR) algorithm [12,13], in order to examine the competing effects of the V_{T}, H_1 and H_2 terms on the system's energy eigenfunctions.

For large tube separations, and in the absence of external fields, the lower excited wavefunctions are localized over each of the two tubes. As d decreases, the states start to overlap and split into double-tube states with even and odd symmetries, in direct analogy to *gerade* and *ungerade* symmetries in molecules [9]. In the limit of weak magnetic fields, for which B can be considered as a perturbation to V_{T}, these double-tube states become gradually modified. In this case, the (linear) H_1 term leading to the Zeeman effect dominates. For a spinless hydrogen atom, H_1 yields an $eBM/2m_{\mathrm{e}}$ energy term, where M, the magnetic quantum number, denotes the eigenvalues of L_z.

Close to the surface of either tube, the screening potential, $V_{\mathrm{s}} \approx 1/4|r-a|$, is equal to $1/4$ the potential of a *two-dimensional* hydrogen atom [14]. When placed in a magnetic field, a system comprised of an electron near a single tube can, therefore, be viewed as a highly magnified two-dimensional hydrogen atom in a magnetic field [15,16]. Likewise, an electron interacting with *two* tubes is an analog to a highly magnified two-dimensional H_2^+ molecule.

The (non-linear) H_2 term of Eq. (4) becomes important if the magnetic field is strong or if the electronic states are significantly extended away from the tubes, as in highly excited TIS [7]. In these cases the electrostatic $V_{\mathrm{T}}(x, y)$ term should constitute a weak perturbation relative to B. When $V_{\mathrm{T}}(x, y)$ is *entirely neglected* our

states become the Landau states of a free electron in an homogeneous magnetic field

$$\Psi_{nlk}(\mathbf{r}) = \mathrm{e}^{\mathrm{i}kz}\mathrm{e}^{\mathrm{i}l\phi}u_{nl}(\rho),$$
$$E_{nlk} = \frac{\hbar^2k^2}{2m_\mathrm{e}} + \frac{eB\hbar}{m_\mathrm{e}}\left(n + \frac{1+l+|l|}{2}\right), \tag{6}$$

where $u_{nl}(\xi) \propto \xi^{|l|/2}\mathrm{e}^{-\xi/2}L_n^{|l|}(\xi)$, $\xi = eB\rho^2/2\hbar$, and $L_n^{|l|}$ are the associated Laguerre polynomials [17], with $n = 0, 1, 2, \ldots$, $l = 0, \pm1, \pm2, \ldots$. We can see that states of the same $|l|$, that differ by the sign of l are separated in energy by $\Delta E = eB\hbar|l|/m_\mathrm{e}$. For $B = 20$ T and $l = 6$ this gives $\Delta E \approx 12$ meV, which is about the same size as the coupling energy of the $l = 6$ state in the single-nanotube case [7]. Thus, the $V_\mathrm{T}(x, y)$ potential cannot be seen here as a weak perturbation, and the two terms compete. Due to the above ΔE shifts, we can observe only Landau-like states with $l < 0$, while the $l > 0$ states are not confined by the $V_\mathrm{T}(x, y)$ potential.

The sense of electron rotation, i.e., the sign of l, is best probed by looking at the current density, given by the quantum mechanical expression [17]

$$\mathbf{J}(x, y) = -\frac{\hbar}{m_\mathrm{e}}\mathrm{Im}[\psi(x, y)\nabla\psi^*(x, y)] - \frac{e}{m_\mathrm{e}}\mathbf{A}|\psi(x, y)|^2. \tag{7}$$

As we increase B or go to higher excited states, we expect to observe a transition from the Zeeman to the Landau limit, in the present system. Moreover, we can see through $\mathbf{J}(x, y)$ the onset of chaotic motion on the orbits.

3. Numerical results

3.1. Case I: $B \neq 0$, $V_\mathrm{a} = 0$

In Fig. 2, we display the dependence of the eigenenergies of an electron in the vicinity of two nanotubes on the magnetic field $B = 0$–35 T for $V_\mathrm{a} = 0$. The two nanotubes of a radius $a = 0.7$ nm are placed $d = 40$ nm apart, at $x = \pm20$ nm. Most of the lower-lying eigenenergies, shown in the left-hand panel, appear as pairs of nearly degenerate *even* and *odd* states with respect to the reflection in the $x = 0$ line. With the relatively coarse Cartesian grid used here (Δ(grid) = 1 nm), no linear Zeeman splitting appears to exist, except in very few states. This is due to an additional artificial potential of a *quartic* symmetry, induced by the grid roughness. Then, the single-tube angular momentum states [7], proportional to $\mathrm{e}^{\pm\mathrm{i}l\phi}$, combine into *split* pairs of double-tube states, proportional to the $\cos(l\phi)$ and $\sin(l\phi)$ functions, that lack the linear Zeeman term. This problem could be avoided by using a much finer grid or by going to bipolar coordinates [9]. However, the high-energy states that are of a larger interest, shown on the right-hand panel of Fig. 2, are typically highly extended and are, therefore, less sensitive to the grid size. These states are strongly affected by the magnetic field, appearing in the H_2 term, and at high fields $B > 20$ T and high quantum numbers $v \gtrsim 100$ a series of 'Landau-type' levels emerges.

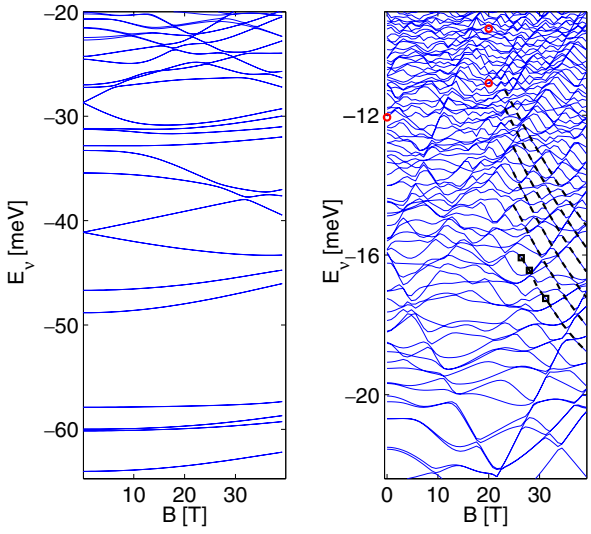

Fig. 2. The dependence of the eigenstates on the magnetic field B, where $V_\mathrm{a} = 0$ and $d = 40$ nm. Eigenstates nos. 33–80 (left panel); eigenstates nos. 75–150 (right panel). The probability-densities of the states marked by circles (squares) are plotted in Fig. 3 top (bottom).

In Fig. 3, we plot probability-densities for several high-energy states, denoted in Fig. 2 by circles (upper panels) and squares (lower panels). Because $V_\mathrm{a} = 0$ the probability-densities are symmetric with respect to $x = 0$. In the absence of external fields, the single-tube image states ($l > 6$) tend to be detached (20–40 nm) from the surface [7]. The presence of a second nanotube breaks the central symmetry of the attractive potential around each of the tubes, and the states collapse on the tube's surface. This is shown on the upper-left panel, where the $v = 120$ state at $B = 0$ resembles the single-tube $l = 6$, $n = 2$ state. (Top middle) As we increase the

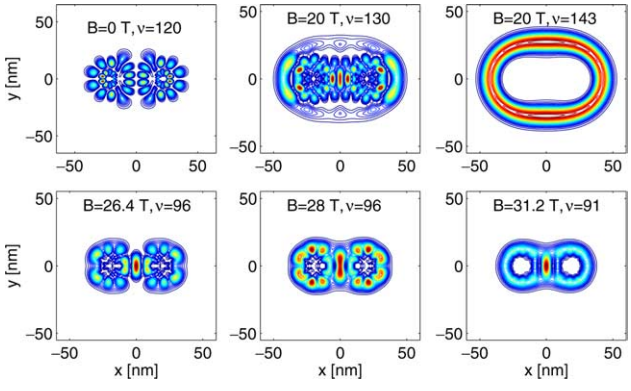

Fig. 3. Contour plots of the probability-density of selected eigenstates for $B \neq 0$ and $V_\mathrm{a} = 0$, showing the formation of 'Landau-like' states.

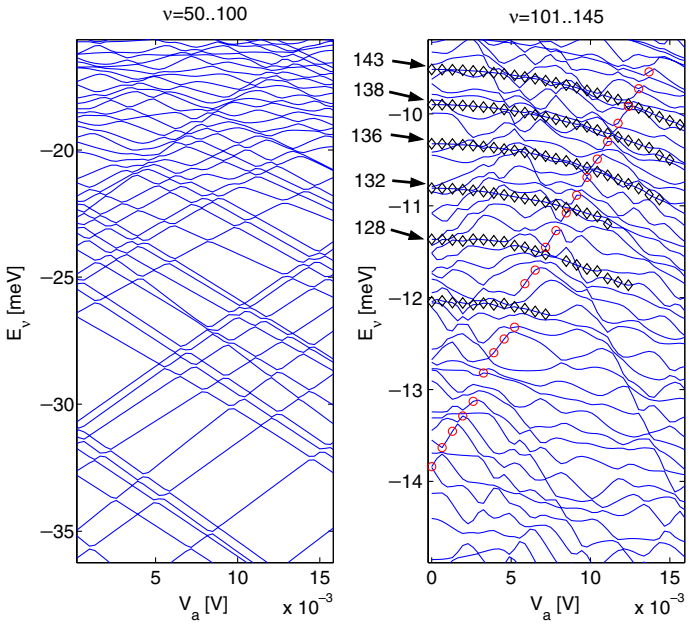

Fig. 4. Dependence of the eigenenergies on V_a, for $B = 20$ T and $d = 40$ nm. Left: Low energy states. Right: High energy states. The ν index designates the positions of some of the ($V_a = 0$) Landau-type states, marked by diamonds.

magnetic field, hybrid states emerge, that show magnetic-free and (detached) Landau-like features. The shown $\nu = 130$ state for $B = 20$ T displays both chaotic nodal patterns [18,19] close to the tube surface, and an extended elliptic-like features ~20 nm away from them. (Top right) Finally, the highly excited $\nu = 143$ state for $B = 20$ T can be described as a perturbed $n = 0$, $l = 25$ Landau state, see Eq. (6), where the numbering comes from the nodal pattern (not shown). Such states are only marginally affected by the presence of the tubes and tend to be completely detached from the tubes' surfaces. As a result, electrons populating them should be protected from the usual annihilation processes occurring on metallic surfaces, which prolongates their lifetimes. Such a situation also occurs in periodic arrays of tubes without the external fields [9]. (Bottom) We also show the evolution of the $\nu = 96$ state with increasing magnetic fields, $B = 26.4$, 28, 31.2 T, with each 'evolution' stage marked by a square in Fig. 2.

3.2. Case II: $B \neq 0$, $V_a \neq 0$

We next introduce the electrostatic potential V_a on the right tube and $-V_a$ on the left tube. In Fig. 4, we show the eigenenergies as a function of V_a, while keeping $B = 20$ T. The low-energy states (left panel) display nearly linear Stark splitting, $E_\nu^\pm = E_\nu^0 \pm \alpha V_a$. The electric field breaks the symmetry of the attractive double-well potential V_T. Thus, for each pair, the lower state localizes around the right, positively charged tube, while the higher state tends to localize around the left, negatively charged tube.

The high-energy spectrum (right panel) is quite complicated. Nevertheless, we can follow series of Landau-like states (marked by diamonds) corresponding to $\nu = 119$, 128, 132, 136, 138, 143. As a general rule, we find that as long as these states maintain their ex-

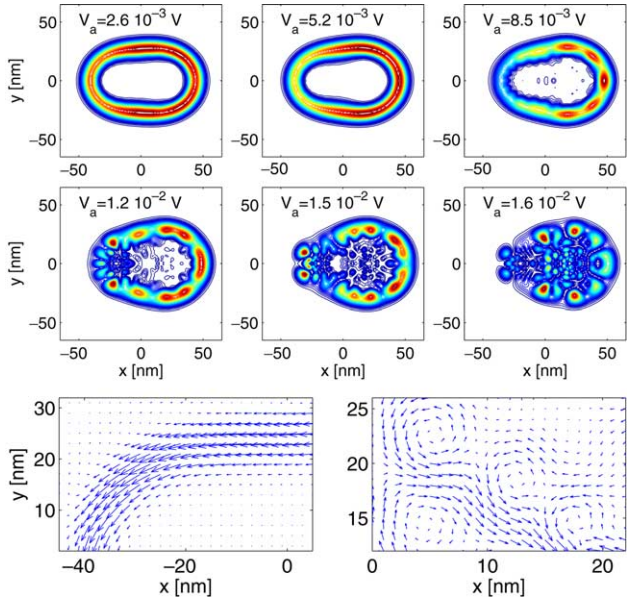

Fig. 5. (Top, middle) The dependence of the probability-density of the $\nu = 143$ state (marked by 'diamonds' in Fig. 4) on V_a, for $B = 20$ T and $d = 40$ nm. Landau-like states at weak electric fields, with ≈27 angular nodes, are seen to collapse on the tubes as V_a is increased. (Bottom) Quiver plot of the current density $\mathbf{J}(x, y)$ calculated from Eq. (7). We plot sections related to two of the probability-densities. (Left panel) $V_a = 2.6 \times 10^{-3}$ V. (Right panel) $V_a = 1.6 \times 10^{-2}$ V.

tended shape, their eigenenergies tend not to vary much with V_a. This is because the energy shifts are compensated, due to the fact that the electron spends in these 'molecular' states about the same time around each of the two oppositely charged tubes, thereby minimizing the linear Stark effect. Similar behavior is observed for a classical electron colliding ballistically with an elliptically shaped quantum antidot [20]. As we increase V_a and the eigenstates start localizing more near one of the tubes (see Fig. 5), their energies are seen to change precipitously. We find an approximate dependence on V_a of the form $E_v \approx 1/(c_1 V_a^2 + c_2)$, where c_1 is the same for different states and $c_2 = 1/E_v^0$. A minority of high-lying eigenenergies sharply increase/decrease with V_a, such as the state shown by circles in Fig. 4. As for low-lying energies, shown in the left-hand panel, these energies correspond to states which are highly localized in the vicinity of only *one* of the tubes. In the regime of high electric ($V_a = 0.04$ V) and magnetic ($B = 30$ T) fields, highly detached states could form exclusively around one of the tubes, or simultaneously collapse on one tube and be detached from the other.

In Fig. 5 (top, middle), we show in details the electric-field induced collapse of the Landau-like state, that occurs as a function of the applied electric field. For small V_a, the probability-density of these extended states is seen to shift to the right. As we increase V_a, these states start to collapse on the surface of the left-hand tube, and become nested around it, while at the same time developing chaotic nodal patterns [18,19]. These are quite consistent with the proliferation of avoided crossings shown in Fig. 4 [21].

The character of the electron motion in this order-chaos transition can be revealed from the current density $\mathbf{J}(x,y)$, in Eq. (7). In the bottom panel of Fig. 5 we show $\mathbf{J}(x,y)$ for states whose probability-densities are plotted in the top-left and middle-right panels, respectively. We find that in the Landau-like state (left) the electron flows regularly counter clockwise around the two tubes, while in the case of the high electric field (right) the current displays vortices associated with the chaotic regime [22,23].

4. Summary

We have demonstrated that image states formed above parallel nanowires can be effectively controlled by the application of mutually perpendicular electric and magnetic fields. In particular, we have clearly seen that Landau-like states, formed in strong magnetic fields, can be gradually changed into chaotic states. Currently, we are examining the relaxation of angular momenta of TIS, leading to the collapse of TIS on the tubes. The process is caused by emission of phonons, giving 'string-like' deformations of the nanowires [24]. We have found that in the absence of external fields the single tube $l = 6 \rightarrow l = 5$ transition is in the 10–100 ps range. Thus, we can anticipate even slower relaxation of angular momenta in the highly extended Landau-like states.

In future, we also plan to study electric and magnetic tuning of image states in periodic systems [25]. Their high sensitivity to the external fields could be used in building of tunable waveguides, mirrors and storage places for low-energy electrons. Such states could be populated by a radiative recombination of the external electrons, where their energy and the light frequency could control the spectrum of populated levels. Image states can also play a role in changing conformations of proteins attached to nanowires [26].

Acknowledgements

This project was supported by a grant from the Feinberg graduate school of the WIS.

References

[1] T. Gallagher, Rydberg Atoms, Cambridge University Press, New York, 1994.
[2] C.H. Greene, A.S. Dickinson, H.R. Sadeghpour, Phys. Rev. Lett. 85 (2000) 2458.
[3] C. Neumann et al., Phys. Rev. Lett. 78 (1997) 4705.
[4] M.G. Gutzwiller, Chaos in Classical and Quantum Mechanics, Springer-Verlag, New York, 1990.
[5] G. Wunner et al., Phys. Rev. Lett. 57 (1986) 3261.
[6] J. von Milczewski, T. Uzer, Phys. Rev. E 55 (1997) 6540.
[7] B.E. Granger, P. Král, H.R. Sadeghpour, M. Shapiro, Phys. Rev. Lett. 89 (2002) 135506.
[8] D. Segal, P. Král, M. Shapiro, Phys. Rev. B 69 (2004) 153405.
[9] D. Segal, B.E. Granger, H.R. Sadeghpour, P. Král, M. Shapiro, submitted.
[10] K. Sasaki, Phys. Rev. B 65 (2002) 195412.
[11] J.C. Slater, N.H. Frank, Electromagnetism, McGraw-Hill, New York, 1947.
[12] D.T. Colbert, W.H. Miller, J. Chem. Phys. 96 (1992) 1982.
[13] R. Guantes, S.C. Farantos, J. Chem. Phys. 113 (2000) 10429.
[14] X.L. Yang, S.H. Guo, F.T. Chan, K.W. Wong, W.Y. Ching, Phys. Rev. A 43 (1991) 1186.
[15] A.H. MacDonald, D.S. Ritchie, Phys. Rev. B 33 (1986) 8336.
[16] J.-L. Zhu, Y. Cheng, J.-J. Xiong, Phys. Rev. B 41 (1990) 10792.
[17] L.D. Landau, E.M. Lifshitz, Quantum Mechanics (Non relativistic Theory), Butterworth-Heinemann, 1998.
[18] R.M. Stratt, N.C. Handy, W.H. Miller, J. Chem. Phys. 71 (1979) 3311.
[19] M. Shapiro, G. Goelman, Phys. Rev. Lett. 53 (1984) 1714.
[20] X. Kleber et al., Phys. Rev. B 54 (1996) 13859.
[21] B.V. Chirikov, J. Stat. Phys. 3 (1971) 307.
[22] A. Vardi, M.Sc. Thesis, The Weizmann Institute, Rehovot, 1994.
[23] Ji. Zhen-Li, K.F. Berggren, Phys. Rev. B 52 (1995) 1745.
[24] D. Segal, P. Král, M. Shapiro, in preparation.
[25] Z.P. Huang et al., Appl. Phys. Lett. 82 (2003) 460.
[26] P. Král, Chem. Phys. Lett. 382 (2003) 399.